

CD44 loss of function sensitizes AML cells to the BCL-2 inhibitor venetoclax by decreasing CXCL12-driven survival cues

Short title: Lack of CD44 sensitizes AML cells to venetoclax

Xiaobing Yu^{1,6§}, Leonel Munoz-Sagredo^{1,5§}, Karolin Streule¹, Patricia Muschong¹, Elisabeth Bayer², Romina J. Walter¹, Julia C. Gutjahr², Richard Greil², Miguel L. Concha⁴, Carsten Müller-Tidow⁶, Tanja N. Hartmann^{2,3} and Véronique Orian-Rousseau^{1*},

¹ Karlsruhe Institute of Technology, Institute of Biological and Chemical Systems- Functional Molecular Systems, Karlsruhe, Germany

² Department of Internal Medicine III with Hematology, Medical Oncology, Haemostaseology, Infectiology and Rheumatology, Oncologic Center, Salzburg Cancer Research Institute - Laboratory for Immunological and Molecular Cancer Research (SCRI-LIMCR), Paracelsus Medical University, Cancer Cluster Salzburg, Salzburg, Austria

³ Department of Internal Medicine I, Faculty of Medicine and Medical Center, University of Freiburg, Freiburg, Germany;

⁴ Institute of Biomedical Sciences, Faculty of Medicine, University of Chile, PO Box 70031, Santiago, Chile. Biomedical Neuroscience Institute, Independencia 1027, Santiago, Chile. Center for Geroscience, Brain Health and Metabolism, Santiago, Chile

⁵ Biomedical research center, Faculty of Medicine, Universidad de Valparaiso, Angamos 680, 2540064 Viña del Mar, Chile

⁶ Department of Medicine, Hematology, Oncology and Rheumatology, Heidelberg University, 69120 Heidelberg, Germany

§: authors contributed equally to the paper

*: **corresponding author:** Véronique Orian-Rousseau, Karlsruhe Institute of Technology- Institute of Biological and Chemical Systems- Functional Molecular Systems, Hermann-von-Helmholtz-Platz 1, 76344 Eggenstein-Leopoldshafen, Germany
veronique.orian-rousseau@kit.edu, Tel: +4972160826523

Key Points:

- CD44 modulates CXCL12-induced stemness features and resistance to venetoclax on AML cells
- CD44 and CXCR4 physically associate at the cell membrane upon CXCL12 induction

Abstract

Acute myeloid leukemia (AML) has a poor prognosis under the current standard of care. In recent years, venetoclax, a BCL-2 inhibitor, was approved to treat patients, ineligible for intensive induction chemotherapy. Complete remission rates with venetoclax-based therapies are, however, hampered by minimal residual disease (MRD) in a proportion of patients, leading to relapse. MRD is due to leukemic stem cells retained in bone marrow protective environments; activation of the CXCL12/CXCR4 pathway was shown to be relevant to this process. An important role is also played by cell adhesion molecules such as CD44, which has been shown to be crucial for AML development.

Here we show that CD44 is involved in CXCL12 promotion of resistance to venetoclax-induced apoptosis in human AML cell lines and AML patient samples which could be abrogated by CD44 knockdown, knockout or blocking with an anti-CD44 antibody. Split-Venus biomolecular fluorescence complementation showed that CD44 and CXCR4 physically associate at the cell membrane upon CXCL12 induction. In the venetoclax-resistant OCI-AML3 cell line, CXCL12 promoted an increase in the proportion of cells expressing high levels of embryonic-stem-cell core transcription factors (ESC-TFs: Sox2, Oct4, Nanog), abrogated by CD44 knockdown. This ESC-TF-expressing subpopulation which could be selected by venetoclax treatment, exhibited a basally-enhanced resistance to apoptosis, and expressed higher levels of CD44. Finally, we developed a novel AML xenograft model in zebrafish, showing that CD44 knockout sensitizes OCI-AML3 cells to venetoclax treatment *in vivo*. Our study shows that CD44 is a potential molecular target to sensitize AML cells to venetoclax-based therapies.

Introduction

Acute myeloid leukemia (AML) is a devastating disease. To aim for complete remission (CR), the standard approach involves intensive induction chemotherapy. The majority of patients are not eligible for this treatment due to its high toxicity. Non-eligible patients receive a palliative lower intensity therapy^[1]. This daunting scenario is being reshaped by the BCL-2 inhibitor, venetoclax (ABT-199). In combination with hypomethylating agents (HMA) or low-dose cytarabine (LDAC), it has achieved CR in trials with patients that were ineligible for intensive induction therapy, refractory or relapsed patients^[2-5]. Given these results, the FDA granted accelerated approval to these regimes for upfront treatment of AML patients ineligible for intensive induction chemotherapy (FDA, November 21, 2018). Nevertheless, approximately 20% of AML patients treated with venetoclax and HMA azacytidine remain refractory, and of patients achieving CR, a proportion of those with measurable minimal residual disease (MRD) relapse^[6]. MRD is supported by a subset of resistant leukemic cells harboring survival advantages and stemness properties^[6,7]. This phenotype is promoted by a protective microenvironment in the bone marrow^[8]. Venetoclax was shown to have a specific effect on leukemic stem cells' (LSC) energy metabolism, enabling targeting of the LSC compartment^[9]. Several clinical trials currently underway, are aimed at improving venetoclax-based regimes through new associations of therapeutic agents^[4,5] and cytogenetic features of resistant subclones to venetoclax-based regimes are beginning to be described^[10].

Of the molecular pathways exploited by LSCs for their survival, the chemokine receptor CXCR4 is prominent in several types of leukemia, while the adhesion molecule CD44 has been shown to be relevant in AML^[8]. CD44 cooperates with CXCR4 for the survival of normal hematopoietic stem cells in the bone marrow niche, rich in their respective ligands, hyaluronan and CXCL12^[11]. CD44 also functions as a coreceptor for CXCR4^[12] and several other receptors, modulating their signaling efficiency^[13]. The role of this molecular interaction in leukemic cell survival upon exposure to venetoclax, remains unexplored.

Here we show that CXCL12/CXCR4 signaling, induction of resistance to venetoclax-induced apoptosis, and stemness marker expression, are dependent on CD44 *in vitro*. In a novel zebrafish intravital imaging xenograft model, we show that the absence of CD44 in AML cells sensitizes them to venetoclax *in vivo*.

Methods

Patient samples

Primary AML cells were obtained from patient bone marrow at the time of diagnosis at the Third Medical Department, Paracelsus Medical University Salzburg, Austria (ethics committee approval number: 415-E/2009/2-2016). Mononuclear cells were isolated with Ficoll density gradient centrifugation and frozen. Patient characteristics are compiled in Table S1.

Human CXCL12/SDF-1 alpha Immunoassay

ELISA assays were performed using the human CXCL12/SDF-1 alpha Quantikine ELISA Kit (R&D Systems) according to the manufacturer's instructions.

Flow cytometry

The OCI-AML3 and Molm13-VR (venetoclax-resistant, see Supplemental Methods) cell lines and the primary cells were incubated with primary monoclonal antibodies (Table S2) or corresponding isotype controls. CD44 and CXCR4 expression and cells expressing d2EGFP (d2EGFP^{pos}) were identified and sorted using a BD FACSAriaTM I and FACSAriaTM Fusion cytometers.

Transient RNA interference and DNA transfection

OCI-AML3 cells were transfected with 5nM siRNA targeting CD44 (pool of two: (5'-CTGAAATTAGGGCCCAATT-3' 5'-AATGGTGCATTTGGTGAAC-3' Qiagen) or control siRNA (pool of two: 5'-UAAUGUAUUGGAACGCAUAUU-3' 5'-AGGUAGUGUAAUCGCCUUGUU-3' Qiagen) using the HiPerFect transfection reagent (Qiagen).

Bimolecular fluorescence complementation (BiFC) assay

CXCR4-VN, CD44-VC and CD44 Δ ect-VC were transfected using ViaFectTM (Promega), into HEK293T cells. 48 hours post-transfection, cells were treated with hyaluronan (200 μ g/ml) or AMD3100 (5 μ M, 10 min) where indicated, or left untreated, and subsequently induced with CXCL12 (200ng/ml, 10 min), followed by 4% paraformaldehyde fixation. Cells transfected only with CXCR4-VN were used as negative controls. Cell nuclei were stained with DAPI (Dako) for 15 minutes. Confocal images (Zeiss LSM 800) were processed using ImageJ (NIH, Bethesda, MD). For fusion proteins and image analysis, see Supplemental Methods. Sequences of the constructs will be provided on request.

PL-SIN-EOS-S(4+)-d2EGFP-SV40-Puro vector subcloning

The pluripotency reporter vector PL-SIN-EOS-S(4+)-EGFP (gift from James Ellis. Addgene plasmid #21317; <http://n2t.net/addgene:21317>; RRID:Addgene_21317)^[14] was modified by replacing EGFP for the unstable d2EGFP (half-life 22 and 2 hours, respectively), and by adding the puromycin resistance gene, expressed under SV40 promoter independently from d2EGFP (see Supplemental Methods).

CRISPR/Cas9 CD44 knockout

CD44 was knocked out by CRISPR/Cas9 in OCI-AML3 cells (OCI-AML3 *CD44KO*) and in Molm13-VR cells (Molm13-VR *CD44KO*) using a lentiviral vector coding for the single guide RNA, hCas9 and puromycin resistance. Control cells were generated with a CRISPR/Cas9 vector containing a scramble sgRNA with no known target in the human genome. For details of the lentiviral transduction protocol and the selection strategy followed, see Supplemental Methods.

Apoptotic assay

Exponentially growing cells were seeded into wells coated with HA or control wells in technical triplicates, and incubated with CXCL12 200ng/ml. After 1 hour, venetoclax 1 μ M dissolved in DMSO or DMSO alone was added. After 4 hours of incubation, the cells were harvested and stained for AnnexinV-FITC (AnnV) and propidium iodide (PI) and analyzed by FACS. The same protocol was used for AML patient samples but with a shorter venetoclax incubation time (3 hours).

Zebrafish xenografts and intravital imaging:

100-150 OCI-AML3 or OCI-AML3 *CD44KO* cells suspended in PBS and stained with CellTraceTM Violet (CTV: Molecular Probes, USA) were injected into the blastoderm of zebrafish embryos 3hpf and incubated at 33°C. After 2 days, the embryos were anaesthetized and injected into the cardinal vein with 0.4nl of venetoclax 2mM mixed with CellEventTM Caspase-3/7 green detection reagent 10 μ M in DMSO, or the latter alone as control. Two hours post injection (hpi), 12 larvae per group were selected for live confocal imaging. Intravital imaging analysis, see Supplemental Methods.

Statistical analysis

Statistics were performed using GraphPad Prism 6 (Graph Pad Software, CA. USA). After a Shapiro-Wilk test for normality, t-test was used to compare the means between two independent groups with normal distribution, and ANOVA with Bonferroni test for more than two groups. Non-normally distributed datasets were analyzed with the rank-sum Wilcoxon's

test or Kruskal-Wallis test, respectively. Using an $\alpha=0.05$, statistical significance was marked as: p-values < 0.05: *, < 0.01: **, < 0.001: *** and < 0.0001: ****.

Results

Expression of CD44 and CXCR4 positively correlate in primary AML cells

In line with previous publications^[16,17], the expression of the chemokine receptor CXCR4, was increased in leukemic cells from AML patients with poor prognosis compared to those with favorable or intermediate characteristics (Figure 1A). CD44 and CXCR4 expression correlated positively (Figure 1B). Representative flow-cytometric dot-plots of four patients are included in Figure S1A. In sera of the same cohort of patients as in Figure 1A and 1B, higher concentrations of CXCL12 were detected relative to healthy donors (Figure 1C). Of note, cells from patient samples express very low levels of the other CXCL12 receptor, CXCR7 (Figure S1B).

CXCL12 promotes resistance of AML cells to venetoclax-induced apoptosis, a process enhanced by hyaluronan

To assess if the correlation between CXCR4 and CD44 could have functional consequences in survival of AML cells, we used resistance to venetoclax-induced apoptosis as an assay.

Compared to control treatment with DMSO (vehicle of venetoclax), venetoclax induced higher levels of cleaved caspase 3 (C-Cas3) in AML cell lines (Figures 2A and S2A). OCI-AML3, a venetoclax-resistant cell line^[18], exposed to CXCL12 prior to venetoclax, showed lower levels of C-Cas3 compared to controls not exposed to CXCL12 (Figure 2A). As hyaluronan (HA) is the main CD44 ligand and a component of the extracellular matrix in the bone marrow where MRD resides, we evaluated its effect in this *in vitro* setting. Combined with CXCL12, HA further decreased the levels of C-Cas 3 upon venetoclax treatment (Figure 2A). Conversely, Molm13, a cell line highly sensitive to venetoclax, was less protected from apoptosis by CXCL12, and/or HA (Figure S2A). AML patient samples from 5 patients (3 with FLT3-internal tandem duplication (FLT3-ITD), recently shown to be associated with venetoclax-resistance^[10]) were seeded into wells coated with HA or control wells, incubated with CXCL12 and subsequently treated with venetoclax (Figure 2B). After 3 hours, the cells were stained with Annexin V-FITC (AnnV) and propidium iodide (PI) and analyzed by flow cytometry. Venetoclax treatment significantly reduced the cell viability in all cases, except in cells seeded on HA and pre-incubated with CXCL12. To evaluate the contribution of cell anchorage to HA to the protective effect of CXCL12, we compared

venetoclax-induced apoptosis in OCI-AML3 cells that adhered to the HA substrate versus the cells that remained in suspension within the same wells. Figure 2C shows a lower number of apoptotic cells in the adherent cell fraction compared to the suspended one, an effect further enhanced by CXCL12. We further found higher MCL-1 mRNA levels, a mechanism of resistance to venetoclax^[18], upon CXCL12 and HA induction in primary AML cells (Figure 2D). These levels were more than one order of magnitude higher than the ones of BCL-2 in these samples (Figure S2Bi). Levels of expression of CXCR4 and CD44 were not affected by CXCL12 and/or HA induction (Figure S2Bii). Taken together, these results show that CXCL12 enhances resistance to venetoclax, an effect boosted by HA.

CD44 modulates the CXCL12 induced resistance to apoptosis

To see if HA exerted its effect through CD44, we knocked down CD44 with siRNA in OCI-AML3 cells. This abolished the protective effect of CXCL12 against venetoclax-induced cleavage of caspase 3, independent of the presence of HA (Figure 3A-C). To confirm these results, we knocked out *CD44* using CRISPR/Cas9 in OCI-AML3 cells (OCI-AML3 *CD44KO* Figure S2Biv left). Cells expressing Cas9 together with a scramble single guide RNA (OCI-AML3 Scr) were used as controls. In OCI-AML3 Scr cells, CXCL12 and/or HA enhanced resistance to venetoclax, seen by higher cell viability measured by flow cytometry after AnnV and PI staining (Figure 3D). In contrast, OCI-AML3 *CD44KO* cells, were sensitized to venetoclax-induced apoptosis, an effect that could not be rescued by treatment with HA or CXCL12, though both factors in combination had a slight effect (Figure 3D). To complement this model, we generated Molm13 venetoclax-resistant cells (Molm13-VR) by culturing them in increasing concentrations of venetoclax for six weeks, and generated Molm13-VR *CD44KO* as well as Molm13-VR Scr by means of CRISPR/Cas9 (Figure S2Bv left). Molm13-VR cells expressed high levels of MCL-1, while the expression of CD44, BCL-2 and BCL-xL remain unchanged (Figure S2C). Apoptosis remained inducible by relatively high concentrations of venetoclax (1 μ M) in these cells, but was significantly reduced by HA and the combination of both (Figure 3E). As in OCI-AML3 cells, CD44 knockout, also dampened this effect. Treatment of Molm13-VR cells with the CXCR4 inhibitors AMD3100 or WZ811, mimicked this effect (Figure 3F), suggesting that the effect of CD44 could be, at least partially, explained by its co-receptor function on CXCR4^[18]. This in turn implies that this function should also be impaired by CD44 blocking antibodies. Therefore, we sought to unbiasedly prove this effect in AML patient samples. Upon treatment with IM7, an antibody against all CD44 isoforms, the combination of CXCL12 and HA could not rescue AML-patient bone marrow derived cells from venetoclax-induced apoptosis, while maintaining its protective effect in the presence of an isotype control antibody (Figure 3G). This result

suggests that a treatment with a CD44 inhibitor could potentially counteract venetoclax resistance induced by factors present in bone marrow niches.

Of note, neither the levels of expression of CXCR4 in OCI-AML3 cells as measured by qPCR (Figure S2Biii) nor its cell surface localization as measured by FACS (Figure S2Biv) were affected by CD44 knockdown (Figure S2Biii) and knockout (Figure S2Biv) respectively. The same is true for Molm13-VR cells (Figure S2Bv right).

A disruption in the balance between pro and anti-apoptotic proteins can lead to cancer cell survival. To study the effect of the CXCL12/CXCR4 axis on this balance we assessed the *BAX/BCL-2* ratio at the mRNA level by qPCR^[19] in OCI-AML3 cells. This ratio was decreased upon CXCL12 induction (Figure 3H), an effect that was also abrogated when CD44 was knocked down by means of siRNA (Figure 3H-I).

CD44 has been involved in cell cycle changes in other types of leukemia^[20,21]. Since an increased percentage of viable cells upon a proapoptotic treatment could be due to enhanced cell survival but also to increased cell proliferation, we assessed the cell cycle status of the AML cell lines upon *CD44* knockout. EdU incorporation experiments in the presence of HA or not, as well as clonogenic assays, revealed that OCI-AML3 *CD44KO* and Molm13-VR *CD44KO* cell lines did not decrease (Figure S3A) but rather had a moderate increase in proliferation rates (clonogenic assays, Figure S3B). In addition, CXCL12 did not induce proliferation of Molm13-VR cells (Figure S3C). This supports the hypothesis that the increased resistance to venetoclax in the presence of CD44 is due to the difference in cell survival.

CD44 modulates CXCR4 signaling induced by CXCL12, being part of a molecular complex at the cell membrane

Upon CXCL12 induction of OCI-AML3 cells *in vitro*, addition of HA augmented ERK phosphorylation in a concentration-dependent manner (Figure 4A). Downregulation of CD44 by siRNA not only abrogated this cooperative effect of HA, but also led to a decrease of CXCL12 induced signaling in the absence of HA (Figure 4B), suggesting that CD44 is required in CXCL12-induced CXCR4 signaling in AML cells, which is favored by, but does not require, CD44-HA binding. Since osteopontin is another ligand of CD44^[22] also present in the bone marrow^[23], we tested its influence on CXCL12-induced ERK activation. We observed no significant change in ERK phosphorylation upon CXCL12 induction after treatment of OCI-AML3 cells with OPN (Figure S4A).

CD44 cooperation with CXCR4 signaling in the absence of HA suggests a potential direct interaction. Using split-Venus bimolecular fluorescence complementation (BiFC), we observed if both receptors formed complexes upon CXCL12 stimulation. We overexpressed

CXCR4 fused to a N-terminal fragment of Venus fluorescent protein (CXCR4-VN) and the standard isoform of CD44 (CD44s) fused to the complementary C-terminal fragment of Venus (CD44s-VC). Both fragments of Venus are non-fluorescent, but in close proximity (7-10 nm) they can complement to reconstitute a functional fluorescent protein^[24,25]. Due to low transfection efficiency of our AML cell lines with these plasmids, we used HEK293T cells as a proof of principle. Upon the addition of CXCL12 to cells co-transfected with CD44s-VC and CXCR4-VN, we detected a strong fluorescent signal at the cell membrane with confocal microscopy (Figure 4C). The mean fluorescence intensity per cell was calculated in four independent experiments (Figure 4C – graph). HA alone did not induce a significantly higher fluorescent signal, and the combination of HA and CXCL12 did not significantly increase the signal compared to CXCL12 alone. Cells transfected only with CXCR4-VN were used as negative controls, while CD44 Δ ect-VC (lacking CD44 extracellular domain), co-transfected with CXCR4-VN was used as a control for possible random interaction in the context of overexpressed molecules (Figure S4B). These results indicate that CXCL12 induces the recruitment of CD44 to CXCR4. The complex formation was decreased upon treatment with AMD3100 (Figure 4C lower panels). We tested the presence of this complex in OCI-AML3 cells by co-immunoprecipitation and detected a CD44 band upon CXCL12 induction in CXCR4 precipitates (Figure S4C).

CD44-CXCR4 cooperation induces stemness marker expression in AML cells upon CXCL12 stimulation

Therapy-resistant cells comprising the MRD deploy stem cell properties to recapitulate the disease upon relapse. As CD44 cooperation with the CXCL12/CXCR4 axis played a role in resistance of AML cells to venetoclax, we investigated its possible association to a stemness phenotype. Operationally defined LSCs can be enriched with the markers CD34⁺CD38⁻^[26], though CD34⁻ LSC populations have also been identified^[27]. CD34⁺CD38⁻ cells usually express the core embryonic stem cells transcription factors (ESC-TFs), Sox2, Oct4, and Nanog^[7, 28, 29]. Since ESC-TFs control a stemness transcriptional program, including their own transcription in a positive feedback loop^[30], we used them as a stemness feature in AML cells. We stably transduced OCI-AML3 cells with a lentiviral fluorescent Sox2/Oct4 reporter – PL-SIN-EOS-C(3+)-EiP^[14] – which allows puromycin-selection of only the cells expressing these factors, finding a significantly higher expression of BCL-2 and CD44 in the selected subpopulation compared to the unselected bulk of parental OCI-AML3 cells (Figure S5A). We modified a similar vector to report for changes in Sox2/Oct4 expression (PL-SIN-EOS-S(4+)-d2EGFP-SV40-Puro) and transduced OCI-AML3 and Molm13-VR cells to detect cells expressing ESC-TFs within the bulk population (Figure

5Ai-iii;5D). CXCL12 induction increased the proportion of the cell subpopulation expressing d2EGFP (d2EGFP^{pos}), and downregulation of CD44 impeded this effect (Figure 5Bi). CXCL12 also induced an increase in mRNA levels of ESC-TFs in OCI-AML3 cells and in primary cells derived from AML-patients (Figures 5Bii-iii). Interestingly, d2EGFP^{pos} cells also expressed approximately two-fold higher mRNA levels of *CD44*, but not of *CXCR4* (Figure 5Ci and S5Aii,iii). Upon CD44 knockdown, transcript levels of ESC-TFs were drastically decreased and were unresponsive to CXCL12 (Figure 5Bii). OCI-AML3-EOS-S(+4)d2EGFP^{pos} cells exhibited significantly higher *BCL-2* mRNA levels, whereas *MCL-1* and *BCL-xL* levels were not significantly higher (Figure 5Ci). However, *MCL-1* was basally expressed at high levels in OCI-AML3 cells, whereas *BCL-2* had a low basal level in this cell line (Figure S5Aii,iii). As with the ESC-TF expression, primary AML cells followed a similar pattern of expression of anti-apoptotic genes, upon induction with CXCL12 (Figure S5Bi,ii). Given this anti-apoptotic gene expression pattern, we hypothesized that treatment of AML cells with venetoclax would increase the proportion of cells expressing the EOS-d2EGFP reporter. Indeed, 16 hours after treatment with venetoclax, we detected a significantly higher proportion of d2EGFP^{pos} cells in both OCI-AML3-EOS-S(+4)d2EGFP as well as in Molm13-VR-EOS-S(+4)d2EGFP cells (Figure 5Cii). In an inverse approach, AML cells sorted for the higher ~20% of d2EGFP fluorescence intensity had a drastically increased resistance to venetoclax-induced apoptosis, especially in Molm13-VR cells, as compared to the lowest ~20% d2EGFP expressing populations (Figure 5D). These experiments show that CD44 is required for the CXCL12/CXCR4 stimulation of an embryonic stem cell program, which in turn upregulates CD44 expression, and is associated with an enhanced venetoclax-resistance phenotype.

CD44 has a relevant role in resistance to venetoclax-induced apoptosis of AML cells *in vivo*

OCI-AML3 cells engrafted in the spleen and bone marrow, or detectable in peripheral blood of NSG mice, 28 days post injection (dpi) into the tail vein, expressed higher CD44 levels compared to their batch of origin *in vitro* (Figure S6A). This effect was most pronounced in cells recovered from the bone marrow (Figure S6B).

To test the role of CD44 in resistance to apoptosis of OCI-AML3 cells *in vivo*, we injected OCI-AML3 *CD44KO* cells or parental cells in NSG mice. At 14 dpi, OCI-AML3 *CD44KO* cells exhibited a significantly lower engraftment rate (Figure S6Di-iii). Since CD44 is required for homing^[31] (Figure S6Div), biasing the read-out of survival and/or proliferation, we established a complementary *in vivo* model in zebrafish that allows similar engraftment rate of both cell lines and intravital imaging upon venetoclax treatment.

OCI-AML3 and OCI-AML3 *CD44KO* cells (Figure S6C) were labeled with CellTrace™ Violet (CTV) and injected into zebrafish embryos at the blastula stage (Figure 6A). Since the cells are injected before the development of the immune system, the xenografted cells are not rejected. At 48 hpf, both cell lines were found mainly in the caudal hematopoietic tissue (CHT^[32]) and in circulation (Figure 6A). At this stage, zebrafish larvae were treated with a single dose of venetoclax injected into the cardinal vein. This rapidly decreased the number of xenografted cells in the CHT compared to vehicle-injected (DMSO) xenografted controls (Figure S7A). We observed OCI-AML3 cells migrating out of the CHT, into the circulation, after engraftment and CTV fluorescence intensity per cell decreased upon the cell division. Therefore, to evaluate the survival of cells that remained engrafted in the CHT after venetoclax injection, we co-injected CellEvent™ Caspase-3/7 green detection reagent, a fluorescent reporter of apoptosis. At 10 hpi of venetoclax, the mean CTV fluorescence in the CHT showed a tendency towards stabilization for the parental OCI-AML3 cell line, while it continued to decrease for the OCI-AML3 *CD44KO* cells (Figure 6 Bi and Bii). Concomitantly, the apoptosis signal showed a steady increase in OCI-AML3 *CD44KO* cells, while decreasing for the parental cell line. This indicates the sensitization of *CD44KO* cells to venetoclax treatment (Figure 6Biii, movies 1 and 2). The increase in green fluorescence intensity did not occur in controls. To evaluate if the increased venetoclax-resistance of the parental OCI-AML3 cells as compared to their *CD44KO* counterparts *in vivo* was related to the expression of stemness markers, we used the EOS-S(4+)d2EGFP reporter and monitored its level of expression in both cell sublines upon serial *in vivo* passages in our zebrafish model. While OCI-AML3-EOS-S(4+)d2EGFP cells had a significant increase in the d2EGFP^{pos} population proportion between the first and the second *in vivo* passage, and was maintained on a third passage, this increase was moderate in the OCI-AML3-EOS-S(4+)d2EGFP *CD44KO* cells during the same period, generating a statistically significant higher expression of the reporter in the CD44-expressing cells (Figure 6C and S7B).

Taken together, these results show a role of CD44 in resistance to venetoclax-induced apoptosis in this *in vivo* model.

To test the relevance of the CD44/CXCR4 axis in the zebrafish *in vivo* model, we combined the injection of venetoclax with AMD3100. Though AMD3100 did not significantly impact cell survival when injected alone, it boosted the effect of venetoclax over the engrafted OCI-AML3 cells, when both drugs were injected in combination (Fig S7Ci,ii).

Discussion

CXCL12 and the CD44-ligand, HA, are expressed in the bone marrow microenvironment that houses MRD after AML treatment^[8], while CXCR4 on AML cells correlate with adverse prognosis^[16,17]. Given the groundbreaking effects of venetoclax in the treatment of AML patients, we used resistance to venetoclax-induced apoptosis to assess the impact of CXCR4-CD44 interaction in AML cell survival. Our results suggest that CXCR4 requires the co-receptor functions of CD44, positioning it as a putative molecular target in AML to enhance venetoclax-based treatment.

The increased survival capabilities of LSCs are the cause of MRD^[33]. In contrast to the AML cell bulk population, quiescent functionally defined LSCs from AML in the bone marrow overexpress BCL-2^[34,35]. It has been demonstrated that CXCL12 stimulation of CXCR4 induces cell survival through BCL-2, among other mechanisms, influencing both BCL-2 function and expression level^[34]. Our CD44 loss-of-function experiments indicate that the pro-survival signaling effects of CXCR4 in AML require CD44. As HA macromers can directly bind to CXCL12^[36], high molecular weight HA may further contribute by CXCL12 accumulation and presentation to the CXCR4/CD44 complex. It has been described that upon CXCR4 stimulation, the Ras/MAPK/ERK and the PI3K/AKT pathways are activated^[37]. Effectors of these pathways phosphorylate BAD^[38], thus preventing its inhibitory binding to BCL-2 and BCL-xL^[39,40]. Specific inhibition of ERK phosphorylation was shown to induce apoptosis in OCI-AML3 cells^[41]. Additionally, the CXCR4 inhibitor BL-8040 was described to decrease ERK and AKT phosphorylation in AML cell lines and peripheral blood samples from AML patients^[35]. This resulted in a significant decrease in the mRNA levels of *BCL-2 in vivo*. This effect was also observed *in vitro* in which *MCL-1* levels were also significantly decreased, synergizing the effect of venetoclax^[34]. In parallel, AML cells in spleen and bone marrow differentiated and underwent apoptosis^[34]. Our results raise the possibility of regulating the CXCL12/CXCR4 pro-survival pathway through CD44.

In the venetoclax-resistant cell line models, OCI-AML3 and Molm13-VR, we observed that CXCL12 increased the proportion of the cell subpopulation expressing ESC-TFs. CD44 knockdown not only abrogated this induction, but also decreased the basal proportion of this subpopulation. In addition, cells selected for the expression of these ESC-TF had higher levels of CD44, but not of CXCR4, thus positioning CD44 in a possible positive feedback loop to maintain this stemness feature, while potentiating resistance to venetoclax-based regimes induced by CXCL12. In AML, expression of the ESC-TFs was significantly higher in the CD34⁺CD38⁻ cell compartment^[7,42], suggesting a role for these transcription factors in leukemic stemness^[7,42]. The addition of these two effects might contribute to MRD (Figure 7). Similarly, self-renewal of cancer stem cells in solid tumors like gliomas, depends on the Sonic Hedgehog-GLI-Nanog axis which is disrupted by inhibition of CXCR4^[43].

The increased proportion of ESC-TF-expressing OCI-AML3 subpopulation induced by the CXCL12/CXCR4/CD44 axis is unlikely to be explained by cell selection, since in the absence of venetoclax, OCI-AML3 cells expressed virtually no signs of spontaneous apoptosis. They might either stimulate an increase in the proliferation rate of cells already expressing the stemness markers or induce ESC-TF *de novo* expression. This last possibility would mean that this axis could be triggering the reprogramming of partially differentiated blasts to express stemness features. This phenomenon, termed cell plasticity, has profound implications for cancers that deploy cellular hierarchies^[44].

Although CD44 has been a longstanding putative molecular target in AML, its study in AML cell survival *in vivo* is hampered by inhibition of cell homing to protective niches upon injection^[27]. We therefore used zebrafish as a complementary *in vivo* AML xenograft model. The use of zebrafish to model the treatment for leukemias and other hematological malignancies has been described before^[45]. However, in AML its use focused exclusively on screening compounds added to swimming water^[46]. The CHT is the organ to which zebrafish blood stem cells migrate and develop at the larval stage^[32,47]. Zebrafish Cxcl12 is expressed in this region, sharing 89% homology in the receptor-binding site with the human ortholog that binds human CXCR4^[48]. Coherently, the injection of a CXCR4 inhibitor in our zebrafish model, decreased survival of OCI-AML3 engrafted cells upon venetoclax treatment. The CHT has been proposed to be a suitable model of cancer cells homing to the bone marrow^[49]. Having achieved a similar engraftment of OCI-AML3 *CD44KO* cells and its parental cell line in our model allowed us to aim for readouts complementary to our mouse model.

Our data suggest the relevance of modulating the CXCL12/CXCR4 axis through CD44 inhibition in AML cells expressing stem cell markers. It will be of interest to explore if the response rates to venetoclax-based therapies correlates to CXCR4/CD44 levels in AML cells. Since MCL-1 inhibition sensitizes OCI-AML3 cells to venetoclax^[32], and CD44 loss of function also affected MCL-1 expression, blocking CD44 may have the dual potential to sensitize cells to venetoclax while also having an impact on stemness.

Acknowledgments

We are very thankful to the IBCS-FMS rodent facility and in particular to S. Huber, S. Müller and S. Schrader. We are also very grateful to N. Borel from the fish facility of IBCS-BIP. We would like to thank Philipp Haitz and Lisa Geiges for their technical help. Work of VOR group is supported by DFG OR124/22-1 and work of TNH is supported by DFG HA8151/3-1.

Authorship

X.Y. and L.M.S. performed most of the experiments, designed experiments, analyzed and interpreted the data

L.M.S. also developed the zebrafish xenograft model and co-wrote the paper

P.M., E.B., K.S., R.J.W. performed several experiments and analyzed the data

J.C.G. designed experiments and analyzed the data

R.G. provided the patient samples and analyzed the data

M.L.C. provided and supervised the stemness reporter vector subcloning

C.MT provided expertise and access to techniques and infrastructure

T.N.H. designed experiments, analyzed the data, was closely involved in the interpretation of data

V.OR. designed the experiments, analyzed the data, interpreted the data and wrote the paper

Disclosure of conflict of interest

C.MT is a member of the advisor board of Pfizer and Janssen-Cilag GmbH. He has received grants and/or investigational medicinal products from Pfizer, Daiichi Sankyo and BioLineRx. He obtained support for his research from Bayer AG.

VOR has shares in the startup company amcure and is a member of the advisory board of amcure. The peptides developed in amcure target CD44v6. CD44v6 is not the subject of this study and the peptides were not use in this paper.

The other authors do not declare any conflict of interest.

References

1. Pollyea, D.A., *Acute myeloid leukemia drug development in the post-venetoclax era.* Am J Hematol, 2019. 94(9): p. 959-962.
2. DiNardo, C.D., et al., *Safety and preliminary efficacy of venetoclax with decitabine or azacitidine in elderly patients with previously untreated acute myeloid leukaemia: a non-randomised, open-label, phase 1b study.* Lancet Oncol, 2018. 19(2): p. 216-228.
3. DiNardo, C.D., et al., *Venetoclax combined with decitabine or azacitidine in treatment-naive, elderly patients with acute myeloid leukemia.* Blood, 2019. 133(1): p. 7-17.
4. Lachowiez, C., C.D. DiNardo, and M. Konopleva, *Venetoclax in acute myeloid leukemia - current and future directions.* Leuk Lymphoma, 2020: p. 1-10.
5. Pollyea, D.A., et al., *Venetoclax for AML: changing the treatment paradigm.* Blood Adv, 2019. 3(24): p. 4326-4335.
6. Jordan, C.T., *Can we selectively target AML stem cells?* Best Pract Res Clin Haematol, 2019. 32(4): p. 101100.
7. Picot, T., et al., *Expression of embryonic stem cell markers in acute myeloid leukemia.* Tumour Biol, 2017. 39(7): p. 1010428317716629.
8. Konopleva, M., et al., *Therapeutic targeting of microenvironmental interactions in leukemia: mechanisms and approaches.* Drug Resist Updat, 2009. 12(4-5): p. 103-13.
9. Pollyea, D.A., et al., *Venetoclax with azacitidine disrupts energy metabolism and targets leukemia stem cells in patients with acute myeloid leukemia.* Nat Med, 2018. 24(12): p. 1859-1866.
10. DiNardo, C.D., et al., *Molecular patterns of response and treatment failure after frontline venetoclax combinations in older patients with AML.* Blood, 2020. 135(11): p. 791-803.
11. Avigdor, A., et al., *CD44 and hyaluronic acid cooperate with SDF-1 in the trafficking of human CD34+ stem/progenitor cells to bone marrow.* Blood, 2004. 103(8): p. 2981-9.
12. Fuchs, K., et al., *Opposing effects of high- and low-molecular weight hyaluronan on CXCL12-induced CXCR4 signaling depend on CD44.* Cell Death Dis, 2013. 4: p. e819.
13. Orian-Rousseau, V., *CD44 Acts as a Signaling Platform Controlling Tumor Progression and Metastasis.* Front Immunol, 2015. 6: p. 154.
14. Hotta, A., et al., *Isolation of human iPS cells using EOS lentiviral vectors to select for pluripotency.* Nat Methods, 2009. 6(5): p. 370-6.
15. Gutjahr, J.C., et al., *Microenvironment-induced CD44v6 promotes early disease progression in chronic lymphocytic leukemia.* Blood, 2018. 131(12): p. 1337-1349.
16. Konoplev, S., et al., *CXC chemokine receptor 4 expression, CXC chemokine receptor 4 activation, and wild-type nucleophosmin are independently associated with unfavorable prognosis in patients with acute myeloid leukemia.* Clin Lymphoma Myeloma Leuk, 2013. 13(6): p. 686-92.
17. Spoo, A.C., et al., *CXCR4 is a prognostic marker in acute myelogenous leukemia.* Blood, 2007. 109(2): p. 786-91.
18. Pan, R., et al., *Selective BCL-2 inhibition by ABT-199 causes on-target cell death in acute myeloid leukemia.* Cancer Discov, 2014. 4(3): p. 362-75.
19. Raisova, M., et al., *The Bax/Bcl-2 ratio determines the susceptibility of human melanoma cells to CD95/Fas-mediated apoptosis.* J Invest Dermatol, 2001. 117(2): p. 333-40.

20. Blacking T., et al., *CD44 is associated with proliferation, rather than a specific cancer stem cell population, in cultured canine cancer cells*. *Veterinary Immunology and Immunopathology*, 2011. 141: p.46–57.
21. Godavarthy P., et al., *The vascular bone marrow niche influences outcome in chronic myeloid leukemia via the E-selectin - SCL/TAL1 - CD44 axis*. *Haematologica*, 2020. 105(1): p. 136-147.
22. Weber G., et al., *Receptor-Ligand Interaction Between CD44 and Osteopontin (Eta-1)*. *Science*, 1996. 271: p. 509-512.
23. Lèvesque J., et al., *The endosteal ‘osteoblastic’ niche and its role in hematopoietic stem cell homing and mobilization*. *Leukemia*, 2010. 24: p. 1979–1992
24. Nagai, T., et al., *A variant of yellow fluorescent protein with fast and efficient maturation for cell-biological applications*. *Nat Biotechnol*, 2002. 20(1): p. 87-90.
25. Shyu, Y.J., et al., *Identification of new fluorescent protein fragments for bimolecular fluorescence complementation analysis under physiological conditions*. *Biotechniques*, 2006. 40(1): p. 61-6.
26. Bonnet, D. and J.E. Dick, *Human acute myeloid leukemia is organized as a hierarchy that originates from a primitive hematopoietic cell*. *Nat Med*, 1997. 3(7): p. 730-7.
27. Moshaver, B., et al., *Identification of a small subpopulation of candidate leukemia-initiating cells in the side population of patients with acute myeloid leukemia*. *Stem Cells*, 2008. 26(12): p. 3059-67.
28. Yin, J.Y., et al., *High expression of OCT4 is frequent and may cause undesirable treatment outcomes in patients with acute myeloid leukemia*. *Tumour Biol*, 2015. 36(12): p. 9711-6.
29. Xu, D.D., et al., *The IGF2/IGF1R/Nanog Signaling Pathway Regulates the Proliferation of Acute Myeloid Leukemia Stem Cells*. *Front Pharmacol*, 2018. 9: p. 687.
30. Boyer, L.A., et al., *Core transcriptional regulatory circuitry in human embryonic stem cells*. *Cell*, 2005. 122(6): p. 947-56.
31. Jin, L., et al., *Targeting of CD44 eradicates human acute myeloid leukemic stem cells*. *Nat Med*, 2006. 12(10): p. 1167-74.
32. Murayama, E., et al., *Tracing hematopoietic precursor migration to successive hematopoietic organs during zebrafish development*. *Immunity*, 2006. 25(6): p. 963-75.
33. van Rhenen, A., et al., *High stem cell frequency in acute myeloid leukemia at diagnosis predicts high minimal residual disease and poor survival*. *Clin Cancer Res*, 2005. 11(18): p. 6520-7.
34. Abraham, M., et al., *The CXCR4 inhibitor BL-8040 induces the apoptosis of AML blasts by downregulating ERK, BCL-2, MCL-1 and cyclin-D1 via altered miR-15a/16-1 expression*. *Leukemia*, 2017. 31(11): p. 2336-2346.
35. Lagadinou, E.D., et al., *BCL-2 inhibition targets oxidative phosphorylation and selectively eradicates quiescent human leukemia stem cells*. *Cell Stem Cell*, 2013. 12(3): p. 329-41.
36. Purcell, B., et al., *Synergistic effects of SDF-1 α chemokine and hyaluronic acid release from degradable hydrogels on directing bone marrow derived cell homing to the myocardium*. *Biomaterials*, 2012. 33(31):p. 7849-57.
37. Pozzobon, T., et al., *CXCR4 signaling in health and disease*. *Immunol Lett*, 2016. 177: p. 6-15.

38. Bonni, A., et al., *Cell survival promoted by the Ras-MAPK signaling pathway by transcription-dependent and -independent mechanisms*. Science, 1999. 286(5443): p. 1358-62.
39. Cantley, L.C., *The phosphoinositide 3-kinase pathway*. Science, 2002. 296(5573): p. 1655-7.
40. Datta, S.R., A. Brunet, and M.E. Greenberg, *Cellular survival: a play in three Akts*. Genes Dev, 1999. 13(22): p. 2905-27.
41. Ricciardi, M.R., et al., *Quantitative single cell determination of ERK phosphorylation and regulation in relapsed and refractory primary acute myeloid leukemia*. Leukemia, 2005. 19(9): p. 1543-9.
42. Picot, T., et al., *Potential Role of OCT4 in Leukemogenesis*. Stem Cells Dev, 2017. 26(22): p. 1637-1647.
43. Fareh, M., et al., *The miR 302-367 cluster drastically affects self-renewal and infiltration properties of glioma-initiating cells through CXCR4 repression and consequent disruption of the SHH-GLI-NANOG network*. Cell Death Differ, 2012. 19(2):p. 232-44.
44. Fumagalli, A., et al., *Plasticity of Lgr5-Negative Cancer Cells Drives Metastasis in Colorectal Cancer*. Cell Stem Cell, 2020.
45. Deveau, A.P., V.L. Bentley, and J.N. Berman, *Using zebrafish models of leukemia to streamline drug screening and discovery*. Exp Hematol, 2017. 45: p. 1-9.
46. Corkery, D.P., G. Dellaire, and J.N. Berman, *Leukaemia xenotransplantation in zebrafish--chemotherapy response assay in vivo*. Br J Haematol, 2011. 153(6): p. 786-9.
47. Kissa, K., et al., *Live imaging of emerging hematopoietic stem cells and early thymus colonization*. Blood, 2008. 111(3): p. 1147-56.
48. Tulotta, C., et al., *Inhibition of signaling between human CXCR4 and zebrafish ligands by the small molecule IT1t impairs the formation of triple-negative breast cancer early metastases in a zebrafish xenograft model*. Dis Model Mech, 2016. 9(2): p. 141-53.
49. Sacco, A., et al., *Cancer Cell Dissemination and Homing to the Bone Marrow in a Zebrafish Model*. Cancer Res, 2016. 76(2): p. 463-71.

Figure Legends

Figure 1. CD44 expression correlates with CXCR4 in AML cells of patients. (A) CXCR4 cell surface expression of primary AML cells from patients with different prognoses (favorable=3, intermediate=15, adverse=10) was determined via flow cytometry (one-way ANOVA with Bonferroni post-test). **(B)** Cell surface expression of CD44 and CXCR4 were correlated (n=39, Pearson's correlation test, $r=0.3971$, $p\text{-value}=0.012$). **(C)** Serum CXCL12 level of AML patients (n=12) as well as healthy donors (n=15) was measured by ELISA (Student's t-test $p\text{-value}=0.0003$).

Figure 2. CXCL12 and hyaluronan (HA) protect AML cells from venetoclax-induced apoptosis.

(A) OCI-AML3 cells were pre-incubated with CXCL12 and/or HA where indicated, followed by venetoclax or solvent (DMSO) treatment. Lysates were probed with the antibodies as indicated in Western Blot. One representative experiment out of 3 experiments is shown. The numbers above the C-Cas3 panel indicate fold changes. β -actin was used as loading control. Three independent experiments were quantified (T-test, p value $^* < 0.05$). **(B)** 2×10^6 /ml primary cells from AML patient samples were seeded into wells coated with hyaluronic acid (HA) or control wells for 30 minutes in technical triplicates, and incubated with CXCL12 200ng/ml. After 1 hour venetoclax $1 \mu\text{M}$ or DMSO (vehicle) was added to the corresponding wells. After 3 hours of incubation the cells were harvested and stained for AnnexinV-FITC (AnnV) and propidium iodide (PI) and analyzed by FACS. Since the frozen patient samples contain a population of PI(+) cells, which cannot be distinguished from PI(+) cells at the end of the experiment, the results were calculated using the percentage of viable cells (Annexin V(-), PI(-)). The value of each sample was expressed as a ratio between the percentage of viable control cells (incubated in the absence of HA and/or CXCL12 and treated with DMSO) and the percentage of viable cells in each of the other conditions of the same patient sample, to normalize for basal differences between samples of different patients. N= 5 patient samples (3 FLT3-ITD, 2 normal) in independent experiments (one-way ANOVA, $p\text{-value} ^* < 0.05$; $^{**} < 0.01$) **(C)** OCI-AML3 cells with/without CXCL12 induction were seeded in HA-coated tissue culture plates, followed by venetoclax treatment. Apoptotic cells (AnnV⁺ cells) of the adherent and suspended populations were determined separately by flow cytometry. Three independent experiments were quantified (one-way ANOVA, $p\text{-value} ^{**} < 0.01$, $^{****} < 0.0001$). **(D)** Primary AML cells were incubated with CXCL12 and/or HA coating for 4 h. mRNA expression of BCL-2 and MCL-1 were determined by qPCR from 3 independent experiments with 3 different primary AML samples (Kruskal-Wallis test $p\text{-value} ^* < 0.05$).

Figure 3. CXCL12 induction of resistance to venetoclax requires CD44 (A-C) OCI-AML3 cells transiently transfected with either CD44 siRNA or control siRNA, were pre-incubated with CXCL12 and/or HA, followed by venetoclax or DMSO treatment. Lysates were probed by Western Blot. One representative experiment out of 3 experiments is shown. β -actin was used as loading control. The numbers above the C-Cas3 panel indicate fold changes. Three independent experiments were quantified (Kruskal-Wallis test, p value $* < 0.05$). **(D)** OCI-AML3 cells and **(E)** venetoclax-resistant Molm13 (Molm13-VR) cells were transduced with CRISPR/CAS 9 lentiviral vectors encoding either scrambled or CD44 sgRNA, followed by puromycin selection and FACS sorting for cells not expressing CD44. Cells with/without CXCL12 induction were seeded in HA or solvent (PBS) -coated tissue culture plate, followed by venetoclax or DMSO treatment. Viable cells were determined by flow cytometry using AnnV and PI staining. One representative experiment out of 3 experiments is shown. (one-way ANOVA, p-value $* < 0.05$, $** < 0.01$, $*** < 0.001$, $**** < 0.0001$). **(F)** Molm13-VR cells were pre-incubated with CXCR4 inhibitors (AMD3100 or WZ811) and induced with CXCL12, followed by venetoclax or DMSO treatment. Viable cells were determined by flow cytometry using AnnV and PI staining (T-test, p value $* < 0.05$). **(G)** Primary AML cells were pre-incubated with an anti-CD44 antibody (IM7) or the corresponding isotype (IgG) seeded in HA-coated tissue culture plates, and induced with CXCL12 (200ng/ml). After 3 hours the cells were stained for AnnV and PI and analyzed by FACS. The results of each patient sample show the percentage of viable cells, normalized as a ratio between control cells (incubated with IgG control and DMSO) and the viable cells in each of the other conditions. N= 4 patient samples (2 FLT3-ITD, 2 normal) in independent experiments. (one-way ANOVA, p-value $* < 0.05$). **(H-I)** OCI-AML3 cells transiently transfected with either CD44 siRNA or control siRNA, were induced with/without CXCL12. mRNA expression of CD44, BCL-2 and BAX were determined by qPCR from 4 independent experiments. Wilcoxon's rank-sum test p-value $* < 0.05$.

Figure 4. CD44s directly interacts with CXCR4 upon CXCL12 stimulus. (A) OCI-AML3 cells were treated with CXCL12 and increasing concentrations of hyaluronan (HA). **(B)** OCI-AML3 cells transiently transfected with CD44 siRNA or control siRNA were treated with CXCL12 (200 ng/ml) and/or HA (200 μ g/ml). ERK phosphorylation was detected using a phospho-ERK-specific antibody by Western blot. One representative experiment out of 3 experiments is shown. Three independent experiments were quantified (Kruskal-Wallis test, p value $* < 0.05$, $** < 0.01$) **(C)** Upper Panel: HEK293T cells were transfected with a plasmid encoding CXCR4 fused with the N-terminal fragment of the Venus fluorescent protein (CXCR4-VN) and with a plasmid encoding CD44 standard fused with the C-terminal domain of Venus (CD44s-VC). The transfected cells were either left uninduced or induced with

CXCL12, HA or a combination of both as indicated. Nuclei were stained with DAPI (blue). The BiFC signal (yellow) was visualized by confocal microscopy (LSM800 Zeiss microscope 63x objective, scale bar=10µm). Mean corrected total cell fluorescence (CTCF) of each cell was analyzed from 4 independent experiments (n=200 cells). Lower Panel: HEK293T cells transfected as indicated above were treated with AMD3100 (5µM, 10 min) or left untreated and subsequently induced with CXCL12 (200 ng/ml, 10 min) or left uninduced. Mean CTCF of approximately 450 cells of each condition from two independent experiments were analyzed (One-way ANOVA): p-value *<0.05, **<0.005, ***<0.0005, ****<0.0001.

Figure 5. Embryonic-stem-cell marker expression in AML cells can be enhanced by CXCL12, depends on CD44 expression, and is associated to apoptosis resistance. (A) OCI-AML3 cells express core embryonic stem cell transcription factors (ESC-TFs). **(i)** Modified version of the PL-SIN-EOS-S(4+)-EGFP pluripotency reporter ^[24] (Addgene MTA (Order 35560), expressing the unstable version of EGFP (d2EGFP: half-life 2 hours), followed by the constitutive promoter SV40 driving the puromycin resistance gene, allowing the selection of cells carrying the reporter independently from their Oct4/Sox2 expression levels. **(ii)** OCI-AML3 cells transduced with the vector described in **(Ai)** OCI-AML3-EOS-S(4+)d2EGFP were analyzed by FACS for the expression of d2EGFP (parental OCI-AML3 cells were used as the negative control for the gating strategy), and **(iii)** sorted for cells expressing the reporter (d2EGFP^{pos}) and cells not expressing it (d2EGFP^{neg}). **(B)** CXCL12 enhanced ESC-TF expression requires CD44. **(i)** OCI-AML3-EOS-S(4+)d2EGFP cells transfected with CD44 siRNA or control siRNA were treated with CXCL12 (200 ng/ml) for 1 h or left untreated. Percentages of d2EGFP^{pos} cells were measured by FACS (Wilcoxon's rank-sum test for 3 independent experiments). **(ii)** Parental OCI-AML3 cells were treated as in **(Bi)** and mRNA levels of the core ESC-TFs was measured by qPCR (one-way ANOVA of 3 independent experiments). **(iii)** Primary cells from three AML patient samples were treated with CXCL12 (200 ng/ml) and mRNA levels of the core ESC-TFs were measured by qPCR. **(C)** **(i)** mRNA levels of CD44, CXCR4 and BCL-2 family members was determined by qPCR and expressed as fold change between cells sorted for d2EGFP expression as in (Aiii). **(ii)** OCI-AML3-EOS-S(4+)d2EGFP and Molm13-EOS-S(4+)d2EGFP cells were treated with venetoclax 3µM for 16 hours and the percentage of d2EGFP^{pos} was measured by FACS. **(D)** Molm13-VR-EOS-S(4+)d2EGFP and OCI-AML3-EOS-S(4+)d2EGFP cells sorted for the ~20% of cells expressing the highest and the ~20% lowest d2EGFP fluorescence intensity, were treated with venetoclax or DMSO. Apoptotic (AnnV⁺/PI⁺) cells were determined using AnnV and PI staining by flow cytometry. Three independent experiments were quantified (T-test, p-value ***<0.001, ****<0.0001).

Figure 6. OCI-AML-3 *CD44KO* xenografted cells are less resistant to apoptosis upon treatment with intravenous venetoclax in an intravital imaging zebrafish model. (A) OCI-AML-3*CD44KO* or its parental cell line was stained with CellTraceTMViolet (CTV), and injected into the inner cell mass of blastula-stage zebrafish embryos. Upon development both cell lines were tolerated and engrafted in the caudal hematopoietic tissue (CHT). At 2 days post cell implantation, engrafted zebrafish larvae were treated with a single dose of 0.4 nl of venetoclax 2 mM, injected into the cardinal vein, in combination with a CellEventTMCaspase3/7 Green Detection fluorescent reagent. At 2, 10 and 20 hpi, intravital confocal images were taken and total CTV (blue) cell fluorescence as well as green fluorescence in the CHT was measured using Image J. **(B) (i)** Representative greyscale pictures of the three time points in the blue channel (CTV) merged with brightfield. **(ii)** Plot of the mean total CTV fluorescence in the CHT. **(iii)** Plot of the mean total fluorescence of the CHT in the green channel (apoptosis reporter), normalized to the total CTV fluorescence in the same area on each xenografted zebrafish larvae (T-test; n=12 engrafted zebrafish larvae per group). Time lapse follow up of individual engrafted zebrafish larvae of both cell sublines can be seen in Supplemental movies. **(C)** OCI-AML3-EOS-S(4+)d2EGFP cells or OCI-AML3-EOS-S(4+)d2EGFP *CD44KO* cells were injected into zebrafish embryos as described above and incubated at 33°C. 3 dpi the zebrafish larvae were sacrificed by ice cold E3 medium after anesthesia with Tricaine. Larvae tails, which contain the CHT were micro-dissected, dissociated by incubation in Trypsin-EDTA, strained through a 40µm mesh, cultured in normal cell conditions. Upon proliferation d2EGFP expression was measured by FACS and the cells were re-implanted into zebrafish embryos initiating the next passage. Representative histograms of one experiment and quantification of 3 sequential *in vivo* passages of 3 independent experiments are shown.

Figure 7. Possible contribution of CXCR4/CD44 for MRD. Our results show that the interaction between CXCR4 and CD44 upon CXCL12 stimulation may contribute to the maintenance of a stem-cell-like phenotype in AML cells by inducing a transcriptional program driven by the core ESC-TFs which promote their own transcription as well as of other stemness target genes.^[26] This upregulates *CD44*, contributing to the maintenance of the phenotype in this environment. In parallel, antiapoptotic protein levels of the BCL-2-family are increased, potentiating resistance to apoptosis induced by venetoclax. Molecule cartoons were taken from ScienceSlides (VisiScience Corp) by licensed user Xiaobing Yu.

Figure 1

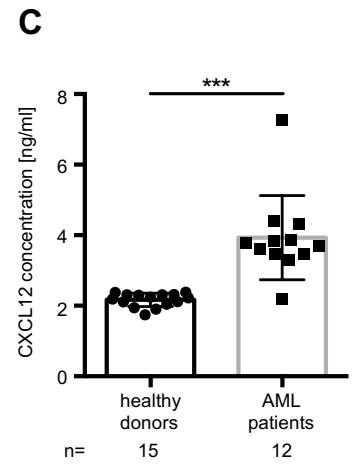
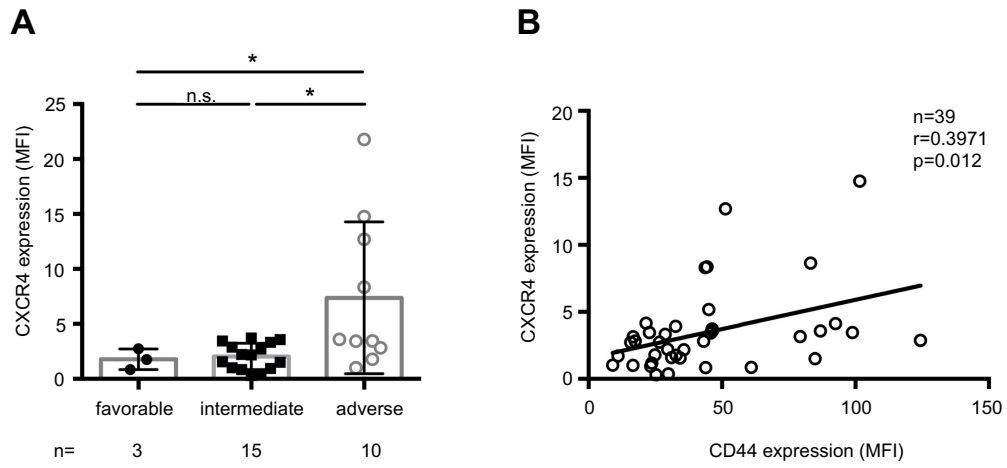


Figure 2

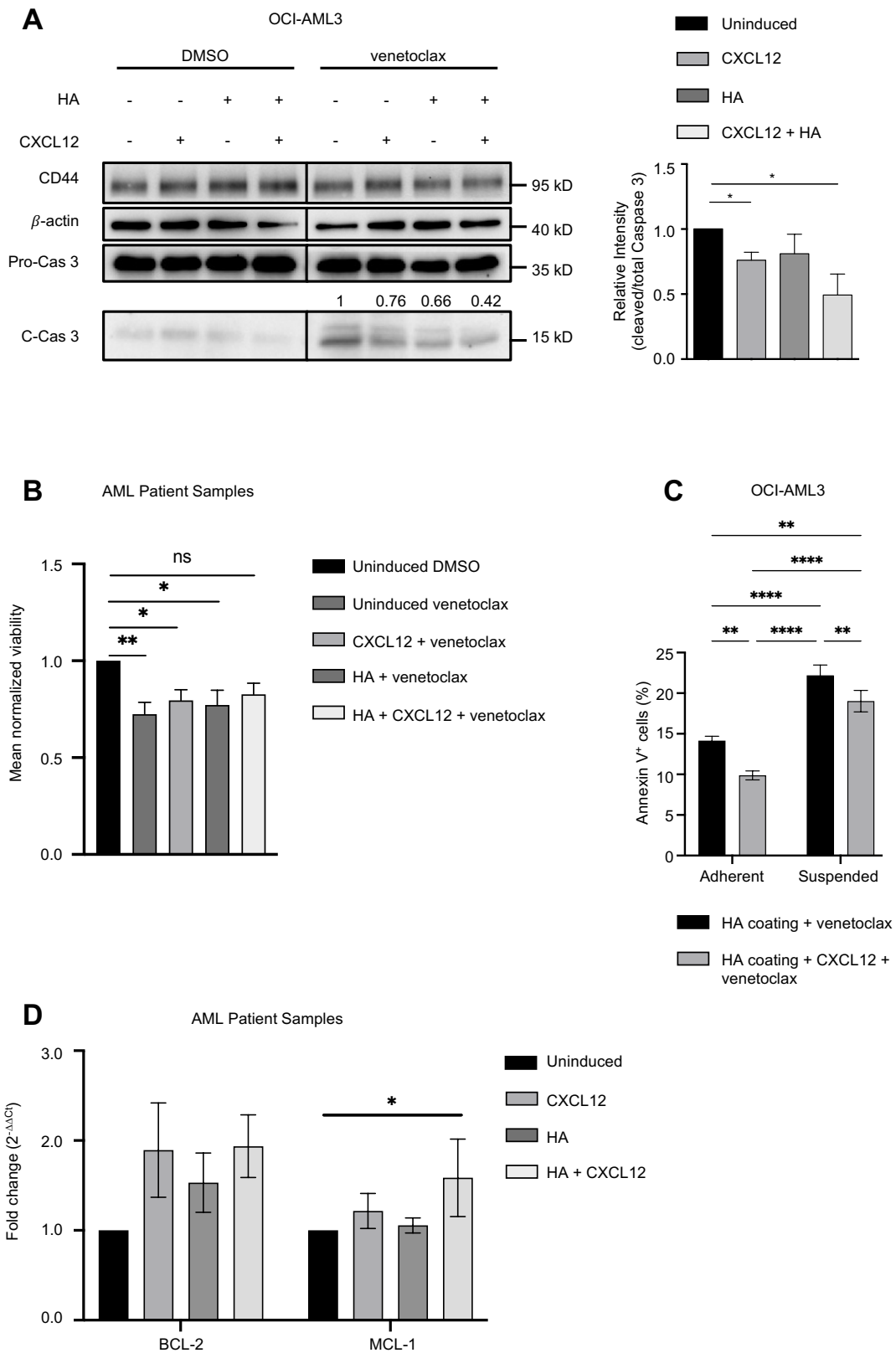


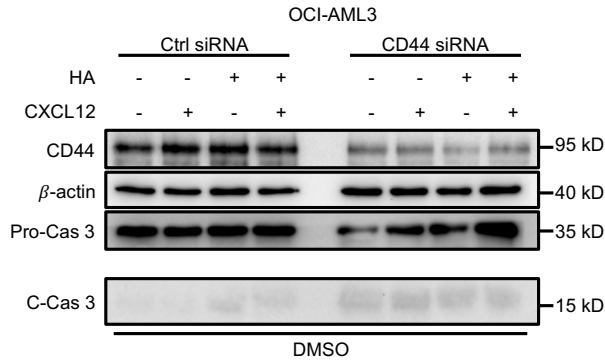
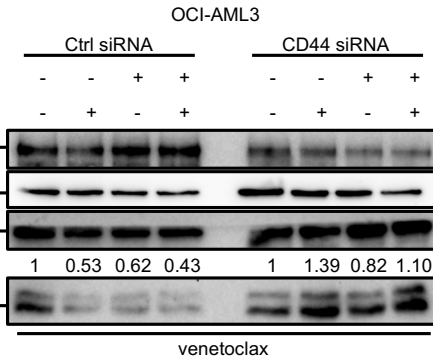
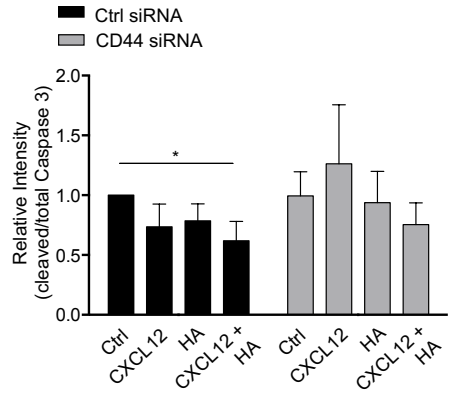
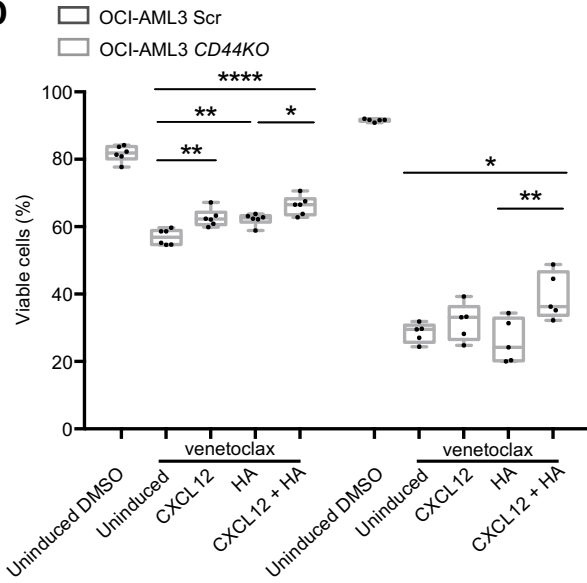
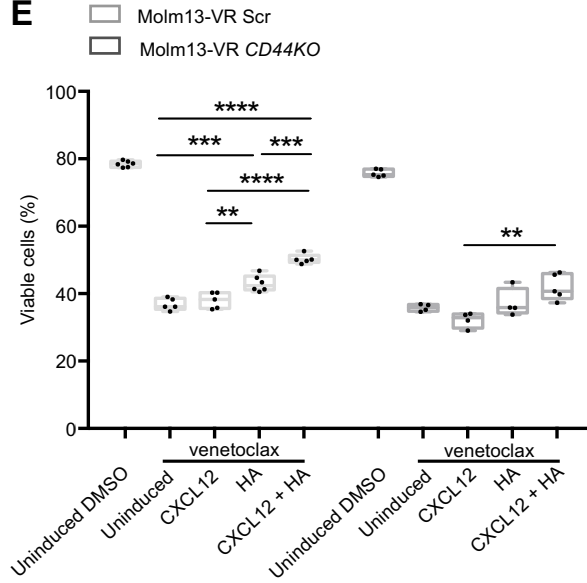
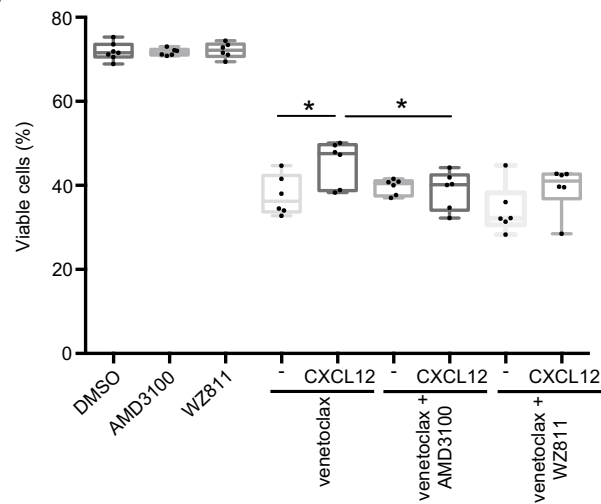
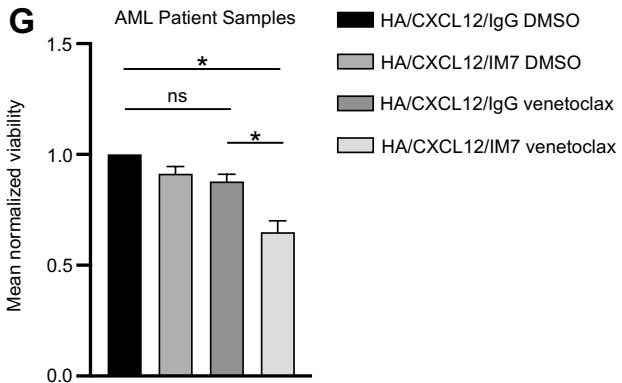
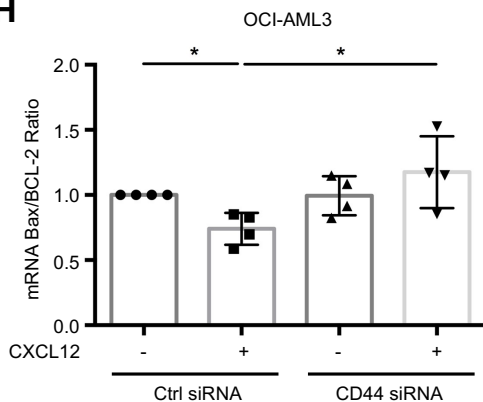
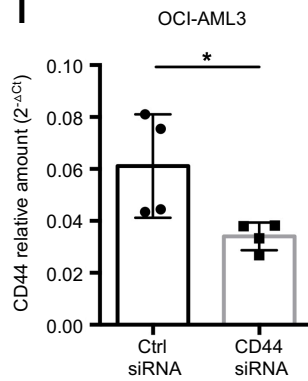
Figure 3**A****B****C****D****E****F****G****H****I**

Figure 4

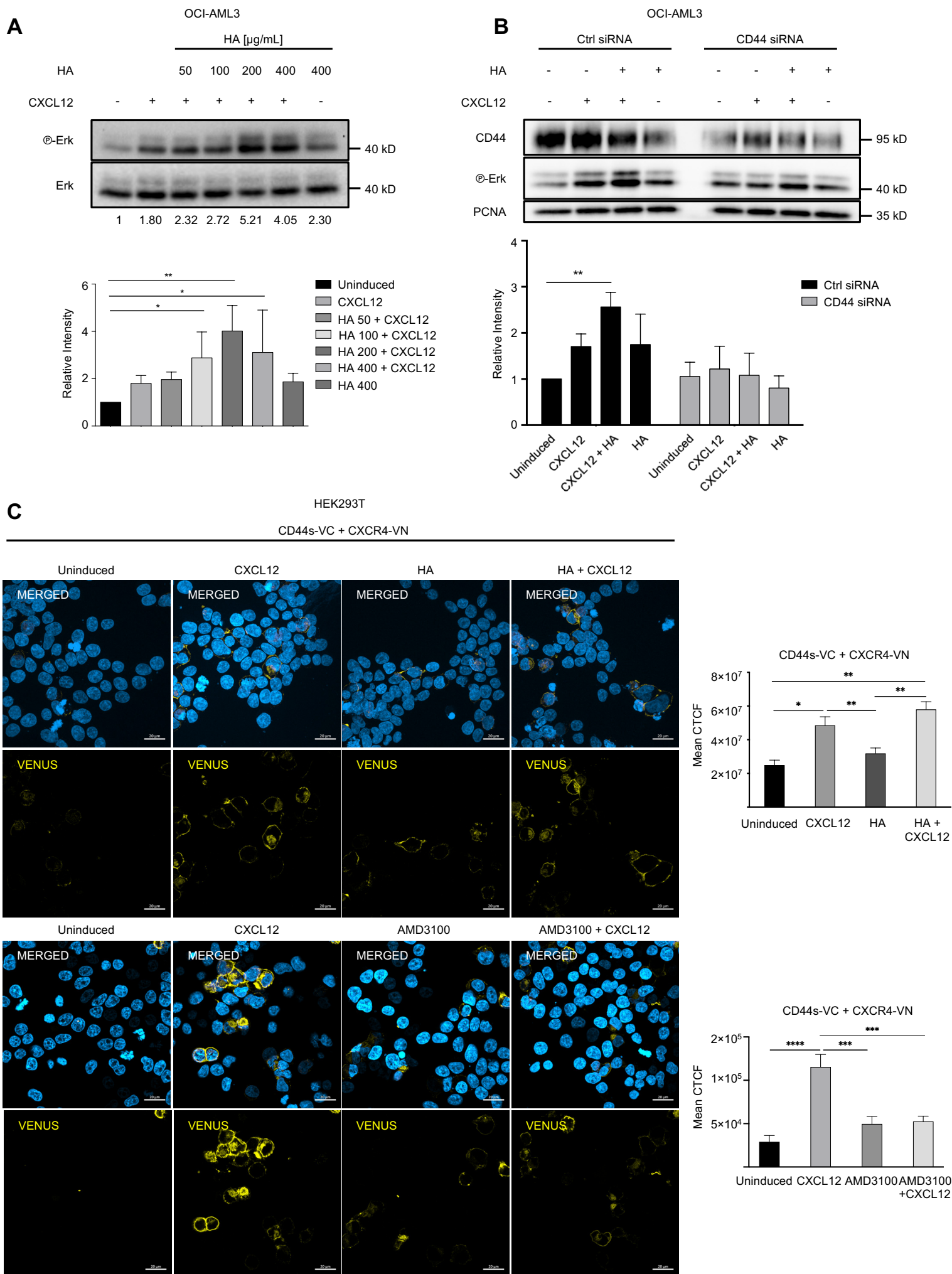


Figure 5

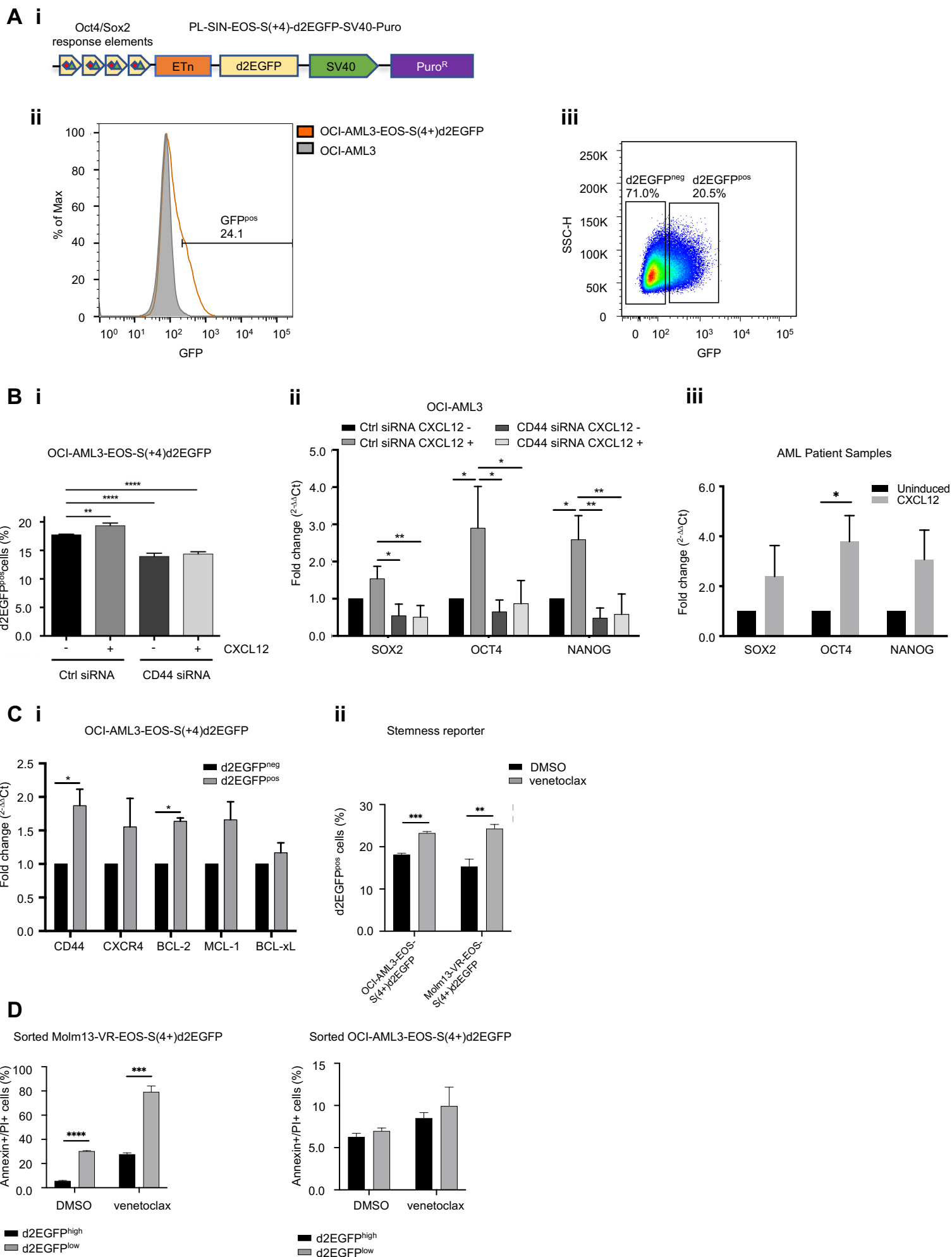


Figure 6

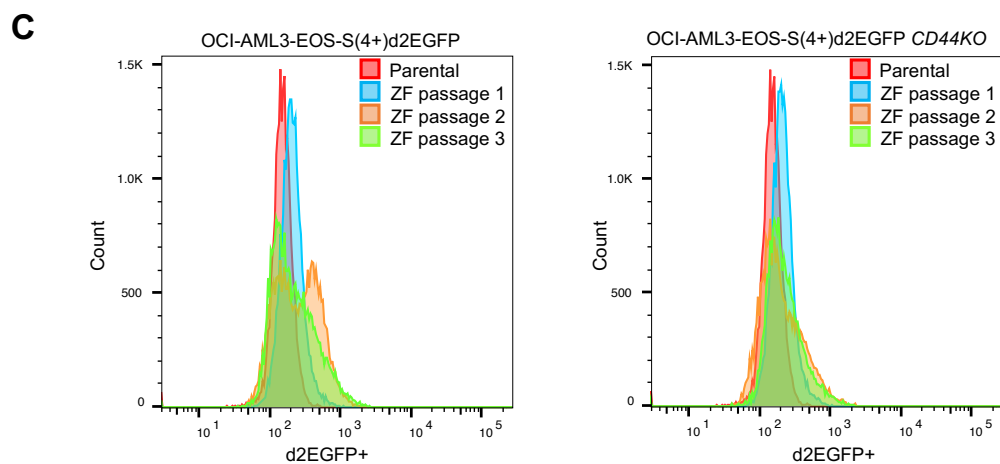
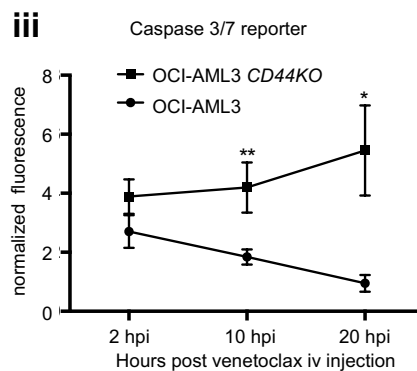
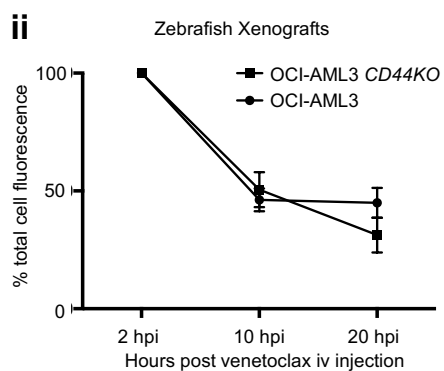
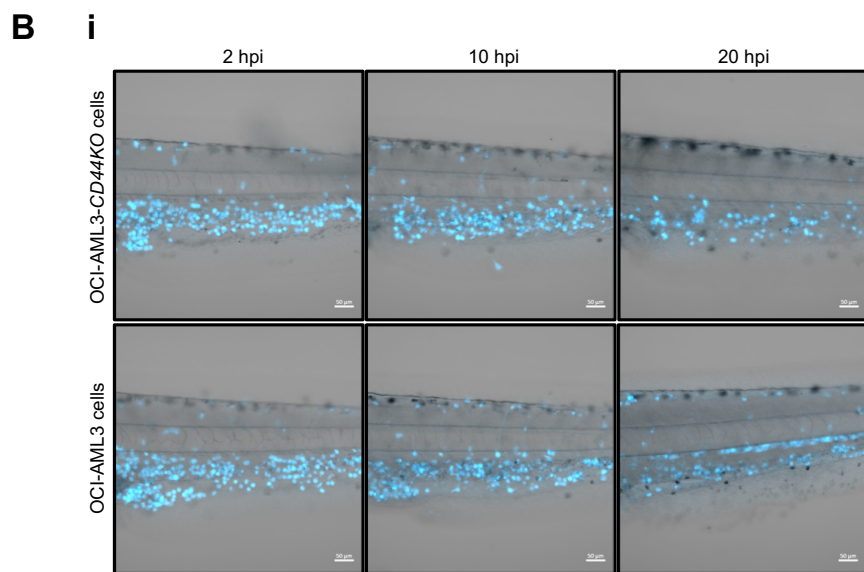
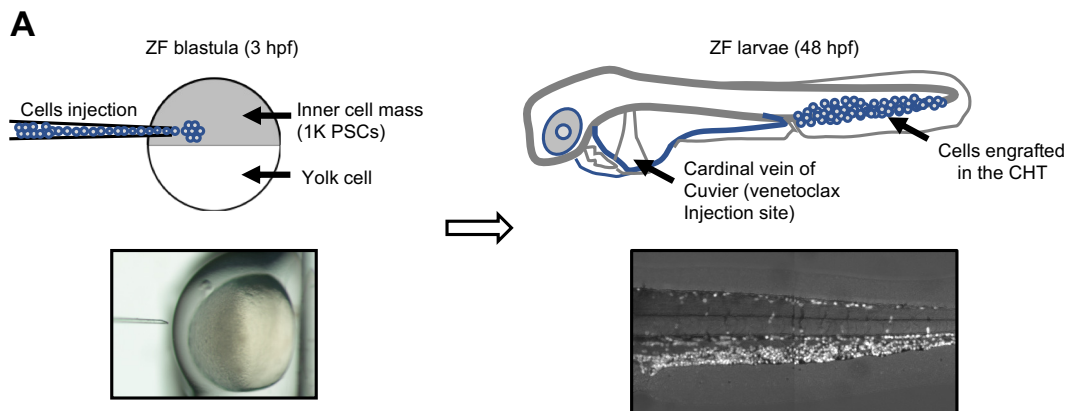


Figure 7

